

2
Conf-9404162--11

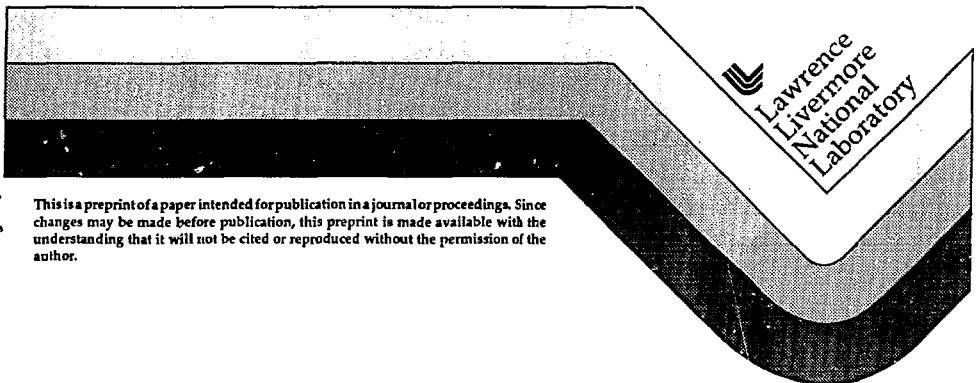
UCRL-JC-118150
PREPRINT

Solid State Frequency Conversion Technology for Remote Sensing

Stephan P. Velsko, Mark S. Webb,
William M. Cook, and William A. Neuman

This paper was prepared for submittal to the
Proceedings of the 1994 CALIOPE ITR Conference
Livermore, California
April 26-28, 1994

July 1994



This is a preprint of a paper intended for publication in a journal or proceedings. Since changes may be made before publication, this preprint is made available with the understanding that it will not be cited or reproduced without the permission of the author.

MASTER

DISTRIBUTION OF THIS DOCUMENT IS UNLIMITED *gts*

DISCLAIMER

This document was prepared as an account of work sponsored by an agency of the United States Government. Neither the United States Government nor the University of California nor any of their employees, makes any warranty, express or implied, or assumes any legal liability or responsibility for the accuracy, completeness, or usefulness of any information, apparatus, product, or process disclosed, or represents that its use would not infringe privately owned rights. Reference herein to any specific commercial products, process, or service by trade name, trademark, manufacturer, or otherwise, does not necessarily constitute or imply its endorsement, recommendation, or favoring by the United States Government or the University of California. The views and opinions of authors expressed herein do not necessarily state or reflect those of the United States Government or the University of California, and shall not be used for advertising or product endorsement purposes.

SOLID STATE FREQUENCY CONVERSION TECHNOLOGY FOR REMOTE SENSING

Stephan P. Velsko, Mark S. Webb, William M. Cook, and William A. Neuman
Lawrence Livermore National Laboratory, P.O. Box 808, L-495, Livermore, CA 94551

1. Introduction

Long range remote sensing from airborne or other highly mobile platforms will require high average power tunable radiation from very compact and efficient laser systems. The solid state laser pumped optical parametric oscillator (OPO) has emerged as a leading candidate for such high average power, widely tunable sources.¹ In contrast to laboratory systems, efficiency and simplicity can be the decisive issues which determine the practicality of a particular airborne remote sensing application. The recent advent of diode laser pumped solid state lasers has produced high average power OPO pump sources which are themselves both compact and efficient.² However, parametric oscillator technology which can efficiently convert the average powers provided by these pump sources remains to be demonstrated. In addition to the average power requirement, many airborne long range sensing tasks will require a high degree of frequency multiplexing to disentangle data from multiple chemical species. A key advantage in system simplicity can be obtained, for example, if a single OPO can produce easily controlled multispectral output. In this paper we will address several topics pertaining to the conversion efficiency, power handling, and multispectral capabilities of OPOs which we are currently investigating. In Section 2, single pulse conversion efficiency issues will be addressed, while average power effects are treated in Section 3. Section 4 is concerned with multispectral performance of a single OPO. The last section contains a short summary and some concluding remarks.

2. OPO Conversion Efficiency and Resonator Design

It is generally appreciated that, in the absence of thermal effects, the efficiency of conversion in a parametric oscillator depends on three factors. The first of these is *pump brightness*, which is directly proportional to the peak power and inversely proportional to a beam quality parameter, such as M^2 . The sensitivity of OPO efficiency to pump brightness depends on the angular sensitivity or walkoff angle of the particular phasematching process involved. Noncritically phasematched processes, with vanishing angular sensitivity and walkoff are the least sensitive to degradations in pump brightness.

The second factor can be denoted as the *dynamic range* effect, and arises most commonly when beams with gaussian spatial or temporal profiles are used as OPO pump sources. If the intensity is adjusted to place the peak of each pulse at the optimum gain, the energy in the *wings* of such pulses will not be converted efficiently. Conversely, if the intensity is adjusted to make the wings closer the optimum gain, at the peak of the pulse the OPO crystal is overdriven, leading to back conversion or worse, to optical damage. Thus, overall conversion efficiency is improved, in principle, if the pump pulse is "square" both in space and time, since only then can the entire beam be converted at the optimum gain value.

The third factor affecting conversion efficiency is the OPO *build-up time*, or, alternatively, the number of round trips the steady-state resonated wave(s) can make during the duration of the pump

pulse. Since the conversion of the pump is small until the resonated wave builds up to approximately the same power as the pump wave, the larger the fraction of the pump pulse which sees the resonated wave at its steady state value, the larger the fraction of pump that will be efficiently converted.

Efficient extraction of energy from solid state lasers in high quality beams usually requires the use of image relayed MOPA configurations or power oscillators with well designed unstable resonators.³ The spatial profiles of MOPA generated beams are ideally supergaussian, as are the output beams of certain unstable resonators. To study the optimization of resonators for OPOs pumped by beams with relatively flat spatial profiles, we have constructed an image relayed Nd:YAG MOPA system with an output of 1J/pulse in 200 nsec pulses at 1.06 μm . By having a large energy and long pulse duration, we obtain reasonable brightness and a large number of round-trip times for typical OPO cavity lengths. We have used this pump to drive a lithium niobate OPO (5 cm long, 47° cut type I, resonating 1.5 μm , idler at 3.7 μm).

Our initial experiments have focused on output coupler optimization and back-conversion effects. Figure 1 shows the pump depletion efficiency as a function of input energy for a 2.9 mm diameter pump beam. Our preliminary hypothesis is that back conversion effects, enhanced by the large circulating resonated wave power present with such high output coupler reflectivities, are the cause of the sharp turnover in conversion efficiency at the higher input energies. It should be noted, however, that the resonator mirrors also have appreciable reflectivities (10–20%) at the 3.6 μm idler wavelength so that partial double resonance character may be affecting the threshold levels and turnover points in this experiment.

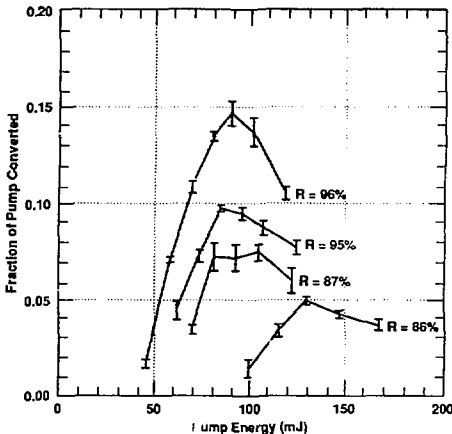


Figure 1. Pump depletion efficiency as a function of input energy.

profile is reminiscent of the lowest order cavity eigenmode of a high Fresnel number flat-flat cavity.⁴ In contrast, Figure 2c shows the spatial profile of the resonated wave for a hemispherical cavity in which the flat high reflector is replaced by a 10 meter curvature spherical mirror. For this cavity, we calculate a lowest order mode diameter of 1.2 mm, close to the observed size of the actual resonated wave.

The hemispherical cavity exhibited a much lower threshold and a much more stable output energy than the flat-flat cavity. Nonetheless, it is clear from Figure 2 that the spatial overlap of resonated wave and pump is considerably smaller for the hemispherical cavity than for the flat-flat cavity. Thus, neither simple cavity design is ideal for efficient extraction of energy from the flat pump beam. We are now turning our attention to a class of imaging *unstable* resonators, such as that shown in Figure 3. In this cavity, effective output coupling for the resonated wave is provided by the magnification of its image (relayed from the pump image plane) on each round trip. The imaging condition is expected to lead to much higher cavity stability in the presence of thermal lensing in the OPO crystal, compared to a conventional non-imaging unstable resonator. Image inversion exerts a smoothing effect on the output beam spatial profile even in the presence of considerable pump non-uniformity. Finally, the ring architecture is advantageous for average power applications because it reduces the thermal load on the OPO crystal from absorption of the resonated wave.

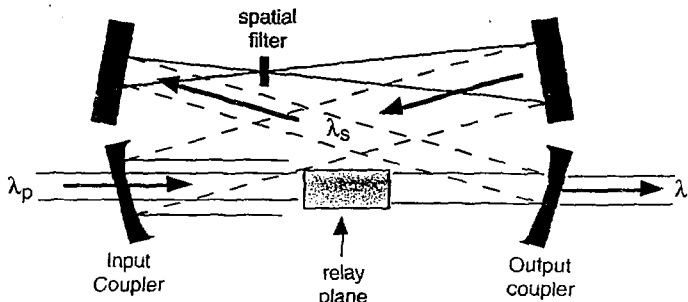


Figure 3. Unstable, self-imaged ring cavity

3. High Average Power Performance of OPOs

Certain long range remote sensing missions may require average power mid-infrared sources in the 10–100 W regime. These power estimates arise from the constraint of high energy per pulse for adequate LIDAR returns coupled with the requirement of high repetition rate for sufficient signal averaging. Such high average powers from an OPO would require a one to two orders of magnitude improvement over existing commercial technology. Even high quality OPO crystals have absorbencies in the 10^{-3} to 10^{-2} cm⁻¹ range within their nominal transparency ranges which give rise to significant thermal loads at pump powers of greater than 10 W.

Figure 2a shows the spatial profile of the pump pulse at the final image plane, which is relayed to the center of our test OPO cavities. We have studied two different cavity types. Figure 2b shows the spatial profile of the resonated wavelength at approximately the same plane as the pump image, obtained with a flat-flat cavity (Fresnel number ≈ 1000). Under these conditions the resonated wave spatial

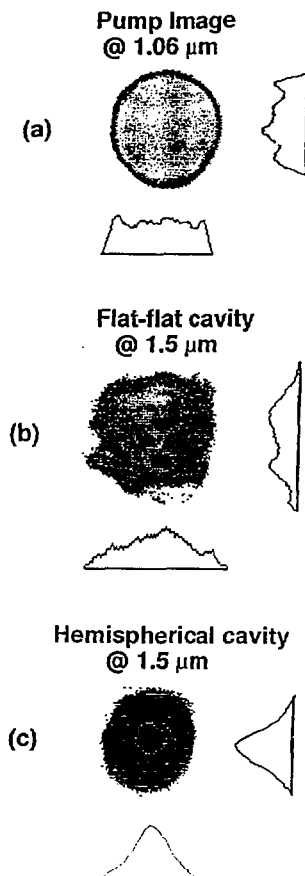


Figure 2. Beam profiles of pump laser, and resonated wave with flat and hemispherical cavities.

The imaging ring architecture described in the previous section represents a potential architectural approach to extending OPO average powers. However, an average power problem more fundamental than thermal lensing effects is the reduction of gain per unit bandwidth across the OPO crystal aperture caused by transverse thermal gradients. In a free running OPO with no spectral narrowing elements, this effect manifests itself as spectral broadening of the OPO output. If gratings or etalons are used to narrow the effective gain bandwidth, or if narrowband seeded operation is desired, thermal gradients will lead to a reduction of conversion efficiency at the desired wavelength.

One possible approach to this problem is "heat capacity limited" operation of the OPO. Here, the crystal is adiabatically mounted to prevent heat flow during operation, and the angle of the crystal is tuned in synchrony with its increasing temperature to maintain the phasematching condition for the desired wavelengths. Clearly, at any instantaneous average power level, the duration of heat capacity operation would be limited by practical considerations such as eventual vignetting or cavity misalignment for large crystal tilt angles. Nonetheless, if the lidar measurement scenario involves only a relatively short "engagement" time with a target, followed by a longer "dead" time in which the crystal is allowed to cool and dissipate thermal gradients, heat capacity limited operation may be useful.

One of the fundamental parameters which determines the average power characteristics of an OPO crystal is the thermal tuning rate, $d\lambda/dT$. This parameter is determined by measuring the change in output wavelength of an OPO whose crystal orientation and pump wavelength are fixed as the temperature of the crystal is changed. Figure 4 shows experimental and calculated thermal tuning behavior of lithium niobate, nominally cut at 47° to the z axis, and pumped with $1.06 \mu\text{m}$. The calculated thermal-tuning curves are based on thermo-optic data from References 5 and 6. The excellent agreement between theory and experiment is somewhat unusual, given the sensitivity of these calculations to the accuracy of the thermo-optic ($d\lambda/dT$) data. The significance of the lithium niobate $4 \text{ cm}^{-1}/^\circ\text{C}$ tuning rate can be understood by considering that an OPO using a typical 5 cm long lithium niobate crystal pumped a few times above threshold has a gain bandwidth of about 1 cm^{-1} . Therefore, the largest tolerable center to edge temperature gradient is around 0.25°C , to remain within the gain bandwidth for a particular fixed frequency. Given an absorption coefficient of 10^{-3} cm^{-1} at $1.06 \mu\text{m}$, this limit would be exceeded at an average pump power of around 80 Watts. Above this power, we would expect to observe reductions in efficiency or loss of spectral purity of a seeded or line narrowed OPO.

Recently, it has been recognized that phasematching orientations with vanishing (first order) thermal tuning rates ($d\lambda/dT = 0$) can be found for certain phasematched three wave mixing processes in biaxial crystals. These orientations exist when the phasematching locus for the process of interest changes shape with temperature, as was shown in Reference 7. An OPO using a crystal cut in such an orientation could tolerate much higher thermal loads, and operate at much higher average powers than would be possible at orientations with non-zero $d\lambda/dT$ values. Using available thermo-optic data, we have searched for such orientations in a number of biaxial nonlinear crystals. It is of considerable interest to note that lithium borate (LBO) does possess thermally insensitive orientations for OPO processes pumped by the Nd:YAG third harmonic at $0.35 \mu\text{m}$. Figure 5 shows the general location of these orientations relative to the principal axes of this crystal. Figure 6 is a plot of the tuning ranges

over which thermally insensitive behavior may be obtained by a combination of angle and temperature changes. Thus, a considerable portion of the visible spectrum can be covered by such an OPO.

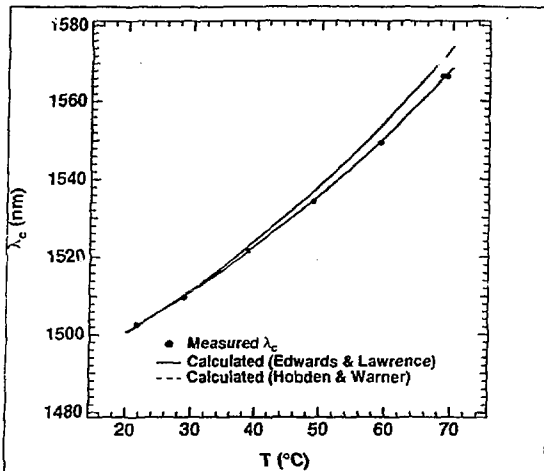


Figure 4. Experimental determination of the thermal tuning rate of lithium niobate, and a comparison with calculations based on thermo-optic data of References 5 and 6.

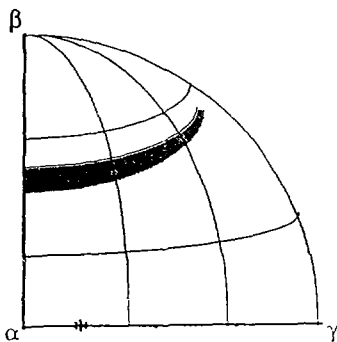


Figure 5. The shaded area represents the range of angles over which a 0.355 μm pumped LBO OPO will exhibit thermally insensitive behavior.

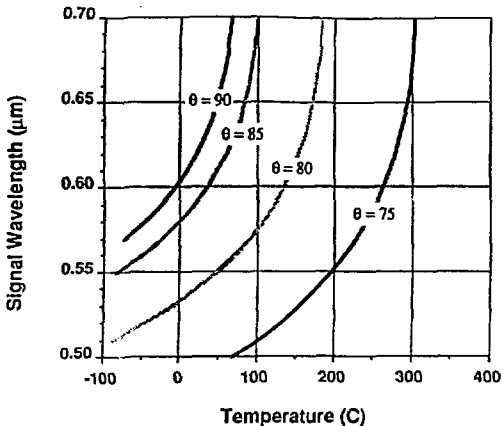


Figure 6. Wavelengths and angles for thermally insensitive OPO action in LBO, at various operating temperatures.

4. Multispectral Parametric Generation and Non-resonant OPOs

Another area of current interest is in the generation of simultaneous multi-line output for mid-infrared DIAL applications. In particular, we have begun to study the properties of the "non-resonant OPO" (NROPO), first described by Guyer and Lowenthal.^{8,9} Figure 7 shows schematically the basic NROPO architecture.

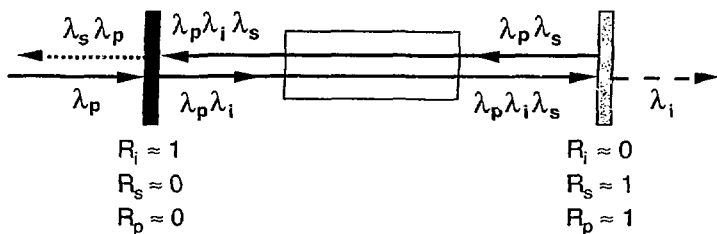


Figure 7. Schematic of the non-resonant OPO. p, s, and i denote pump, signal and idler respectively, and R is the mirror reflectance.

Figure 8 shows the results of a steady-state plane wave calculation of pump depletion efficiency for an idealized NROPO compared to a singly resonant OPO (SRO). Within the plane wave theory, the NROPO has a threshold drive which is equivalent to a SRO with a 50% output coupler.

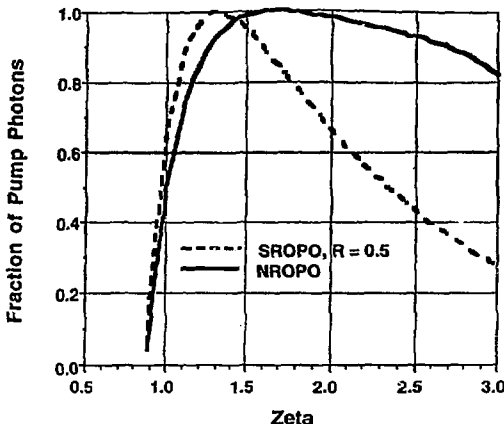


Figure 8. Plane wave calculations of NROPO and SROPO conversion efficiencies. Zeta is the drive parameter $z = CL^{1/2}$, with C = nonlinear coupling parameter, L = crystal length, and I = pump irradiance.

The most compelling property of this device is that it provides high regenerative parametric amplification without cavity resonances. We are planning to investigate whether seed light with arbitrary spectral content can be regeneratively amplified without distortion, within the gain bandwidth of the NROPO device. Our initial experiments will utilize dual frequency seeding based on frequency stabilized tunable diode lasers. Figure 9 shows the basic setup for this experiment. In fact, simple plane wave calculations for the seeded NROPO imply that multiwavelength seeding is expected to generate sidebands under high drive conditions. Figure 10 shows the spectra generated for different values of angle detuning of the nonlinear crystal (lithium niobate) when two waves separated by 5 GHz are injected into an NROPO driven by a 300 mJ, 20 nsec pump pulse. Note that approximately 20% of the generated light is contained in sidebands up to 20 GHz away from the two desired wavelengths. This effect is an intrinsic consequence of the coupled three-wave mixing process, and is probably difficult to suppress completely when significant pump depletion (*i.e.* high conversion efficiency) is desired. The extent to which this effect persists under real experimental conditions (partially divergent pump beams, imperfect mirror reflectivities, etc.) remains to be determined.

5. Concluding Remarks

To a large extent, past work on parametric oscillators for remote sensing and or other spectroscopic applications has not focused seriously on the issues of efficiency and average power. In addition, no precedents exist for the generation of controlled multispectral output from a single OPO. However, substantial progress in these areas will be necessary before a truly compact, highly efficient, multifre-

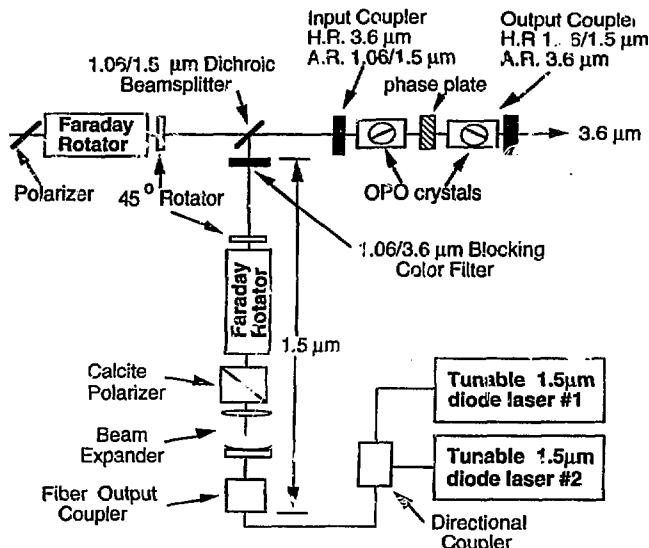


Figure 9. Experimental arrangement for dual wavelength seeding of a 1.06 mm pumped non-resonant OPO.

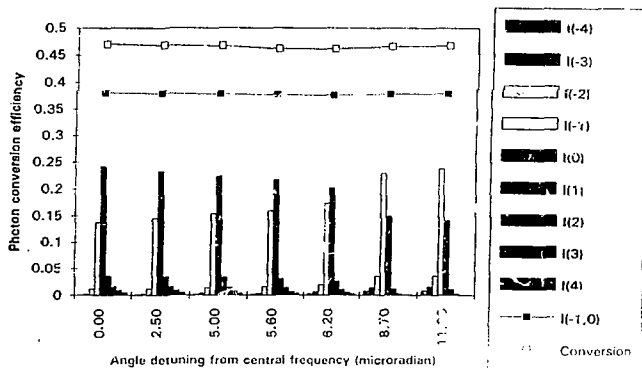


Figure 10. Sideband generation in a dual wavelength seeded NROPO. \square = total pump depletion efficiency, \blacksquare = fraction of power converted to the two seed wavelengths.

quency capable, long range lidar system can be developed for airborne deployment. We anticipate that, in the future, advanced resonators, thermally insensitive materials, and multispectral seeding will be combined with diode pumped solid state pump lasers to realize such a system.

Acknowledgment

This work was performed under the auspices of the U.S. Department of Energy by Lawrence Livermore National Laboratory under Contract No. W-7405-ENG-48.

6. References

1. R. M. Measures, *Laser Remote Sensing* (Krieger Publishing Co., Malabar, Florida, 1992).
2. S. Velsko, C. Ebbers, B. Comiskey, G. F. Albrecht, and S. Mitchell, *App. Phys. Lett.* **64**, 1 (1994).
3. A. E. Siegman, *Lasers* (University Science Books, Mill Valley, California).
4. H. Kogelnik and T. Li, *Applied Optics* **5**, 1550-1567 (1966).
5. M.V. Hobden and J. Warner, *Phys. Lett.* **22**, 243 (1966).
6. G.J. Edwards and M. Lawrence, *Opt. Quantum Electron.* **16**, 373 (1984).
7. C. E. Barker, D. Eimerl, and S. P. Velsko, *J. Opt. Soc. Am. B* **8**, 2481 (1991).
8. D. Guyer and D. Lowenthal, *Proc. SPIE* **1220**, 41-44 (1990).
9. D. Guyer, "High output coupling cavity design for optical parametric oscillators," U.S. Patent No. 5,079,445 (1992).